The Canadian Mineralogist
Vol. 46, pp. 635-650 (2008)
DOI: 10.3749/canmin.46.3.635

PHOSPHATE ASSEMBLAGES FROM THE BRISSAGO GRANITIC PEGMATITE, WESTERN SOUTHERN ALPS, SWITZERLAND

PIETRO VIGNOLA§

CNR – Istituto per la dinamica dei processi ambientali, Operative Unit of Milano, via Mario Bianco 9, I–20131 Milano, Italy

VALERIA DIELLA

CNR – Istituto per la dinamica dei processi ambientali, Operative Unit of Milano, via Botticelli 23, I–20133 Milano, Italy

PAOLO OPPIZZI

Parco delle Gole della Breggia, Casella postale 8, CH–6834 Morbio Inferiore, Switzerland

MASSIMO TIEPOLO

CNR – Istituto di Geoscienze e Georisorse, Operative Unit of Pavia, via Ferrata, 1, I–27100 Pavia, Italy

STEFAN WEISS

LAPIS magazine, Orleansstr. 69, DE–81667 Munich, Germany

ABSTRACT

We describe a first significant occurrence of graftonite–triphylite-bearing LCT-type granitic pegmatite in the Alps. In 1999, in the Brissago area, in the western Southern Alps, Canton Ticino, Switzerland, we found a boulder containing an almost complete section of a phosphate-bearing pegmatite dike. The zoned pegmatite is composed by four main units: 1) an aplite unit, 2) a plagioclase + quartz graphic unit, 3) a coarse-grained plagioclase unit, and 4) a quartz core containing several phosphate masses up to 10 cm in diameter. On the basis of textural features and results of chemical analyses, we distinguish two phosphate associations. Association I, of magmatic origin, is represented by lamellar intergrowths of graftonite and triphylite. The leaching of Li and oxidation of Fe have led to the formation of ferrisicklerite and heterosite in replacement of triphylite, whereas the origin of kryzhanovskite and stanĕkite remains unclear. Association II, of metamorphic origin, consists of a polycrystalline aggregate of graftonite and triphylite. Exceptionally, primary maghagendorfite grains are present. Non-oxidizing low-temperature processes led to the formation of ludlamite and vivianite in replacement of triphylite. Locally, at the rim of phosphate masses, in close association with apatite-(CaOH), jahnsite and mitridatite formed at the expenses of graftonite. The chemical characteristics of the phosphate assemblages and associated mafic silicates indicate that this phosphate-bearing pegmatite dike belongs to a geochemically primitive system. Our U/Pb dating of zircon (242 ± 2.8 Ma) allows us to relate the formation of this dike to the Mid-Triassic tectonomagmatic cycle, characterized by the evolution of a magmatic arc well represented in the Southern Alps. In this geodynamic environment, a pegmatite-forming melt formed after partial melting of metapelites belonging to the Kinzigitic Complex of the Ivrea–Verbano zone.

Keywords: granitic pegmatite, LCT type, phosphates, chemical data, graftonite, triphylite, Brissago, Switzerland.

SOMMAIRE

Nous décrivons un premier indice important d'une pegmatite granitique de type LCT à graftonite + triphylite dans les Alpes. En 1999, nous avons découvert, dans la région de Brissago, dans le secteur occidental des Alpes du Sud, canton du Tessin, en Suisse, un bloc contenant une section presque complète d'un filon pegmatitique porteur de phosphates. La pegmatite zonée comprend quatre unités principales: 1) une aplite, 2) une unité à plagioclase + quartz graphique, 3) une unité riche en plagioclase à grains grossiers, et 4) un noyau de quartz contenant plusieurs masses de phosphate atteignant 10 cm de diamètre.

§ *E-mail address*: pietro.vignola@idpa.cnr.it

A la lumière des aspects texturaux et des résultats d'analyses chimiques, nous distinguons deux associations de phosphates. L'association I, d'origine magmatique, est représentée par des intercroissances lamellaires de graftonite et triphylite. Le lessivage du Li et l'oxydation du fer ont mené à la formation de la ferrisicklerite et de l'hétérosite en replacement de la triphylite, tandis que l'origine de la kryzhanovskite et de la staněkite demeure obscure. L'association II, d'origine métamorphique, est faite de graftonite et de triphylite en agrégats polycristallins. Il est exceptionnel de trouver la maghagendorfite primaire. Des processus de faible température sans tendances oxydantes ont mené à la formation de la ludlamite et de la vivianite en remplacement de la triphylite. Localement, en bordure des masses de phosphates, et étroitement associée à l'apatite-(CaOH), jahnsite et mitridatite se sont formées aux dépens de la graftonite. Les caractéristiques chimiques des assemblages de phosphates et des minéraux mafiques associés indiquent qu'il s'agit d'une pegmatite géochimiquement relativement primitive. Notre datation U/Pb du zircon (242 ± 2.8 Ma) nous permet d'attribuer la formation de ce filon au cycle tectonomagmatique du Triassique moyen, et à l'évolution d'un arc magmatique bien représenté dans les Alpes du Sud. Dans ce milieu géodynamique, un magma granitique propice à la formation d'une pegmatite s'est formé suite à la fusion partielle de métapélites faisant partie du complexe de kinzigites de la zone de Ivrea–Verbano.

(Traduit par la Rédaction)

Mots-clés: pegmatite granitique, type LCT, phosphates, données chimiques, graftonite, triphylite, Brissago, Suisse.

Introduction

Minerals of the graftonite [$(Fe,Mn,Ca)_3(PO_4)_2$] – beusite [$(Mn,Fe,Ca,Mg)_3(PO_4)_2$] and the triphylite [$LiFePO_4$] – lithiophilite [$LiMnPO_4$] series are relatively rare accessory phases of granitic pegmatites. These phosphates are typical of LCT-type pegmatites, in particular in the more evolved portions of the dikes, such as in the intermediate and core-margin zones (Simmons *et al.* 2003).

The first descriptions of these phosphates in the granitic pegmatites of Brissago (Cantone Ticino, Switzerland) are due to De Quervain (1932) and Walter (1950); they reported the presence of graftonite as masses up to 10 cm in length, and microcrystals of hydrothermal phosphates lining cavities in pegmatite boulders. The mineralogical association of these pegmatites has been studied in more detail by Nyffeler (1972) and successively by Weiss (1982, 1985, 1989), Cavalli (1984) and Meisser & Vanini (1997). Weiss *et al.* (2004) produced a review of the phosphate mineralogy of the Brissago area. Up until now, the phosphate masses have only been found in small or very small boulders representing incomplete portions of the original dikes. A prospecting program conducted in 1999–2001 by two of the authors (P.O. and S.W.) led to the discovery of a boulder containing several huge masses of phosphates and a quite complete section of the original dike (Weiss *et al.* 2004). The dike, hosted by the Kinzigitic Complex belonging to the Ivrea Verbano Zone (crystalline basement of the Southern Alps), shows an asymmetrical zoned structure.

The abundance of phosphate masses and other accessory minerals within a complete section of the hosting pegmatite dike permitted a detailed study of the association, and of textural and chemical features of the assemblage of phosphate minerals. The textural and chemical characterization of phosphate masses allows us to infer the degree of evolution of pegmatite-forming melt, the crystallization processes of primary phosphates, and the hydrothermal medium- to low-temperature evolution of the phosphate assemblage. Finally, geochronological data allow us to assess the geodynamic environment of pegmatite crystallization and to make a hypothesis about the source of pegmatite-forming melt.

Geological Framework

The post-Variscan evolution of the central and western basement of the Southern Alps is characterized by three main tectono-magmatic cycles. During the first one, in the Early Permian, mafic intrusive bodies (*e.g.,* the Ivrea gabbro) were emplaced in the lower part of the continental crust, whereas anorogenic (A-type) granitic plutons (*e.g.,* Baveno) and granophyric laccoliths (Cuasso al Monte) and niobium–yttrium–fluorine (NYF) granitic pegmatites were emplaced in the upper crust (Boriani *et al.* 1992, Pezzotta *et al.* 2005) (Fig. 1).

The second cycle, documented by amphibolite-facies LP–HT metamorphic conditions in the basement of the western and central Southern Alps (Ivrea–Verbano Zone and Serie dei Laghi), occurred during a rifting event of Middle to Late Triassic age (Siletto *et al.* 1993, Bertotti *et al.* 1999). The Mid-Triassic geological evolution of the western Southern Alps was characterized by the evolution of a magmatic arc, as indicated by widespread emplacement of andesitic to rhyodacitic volcanic and subvolcanic rocks (Marinelli *et al.* 1980, Garzanti 1985, Stampfli *et al.* 1991). In this period, swarms of granitic pegmatites were emplaced into the middle crust of the Southern Alps (Sanders *et al.* 1996, Bertotti *et al.* 1999, Garzanti *et al.* 2006). This volcanic stage ended in Late Carnian times (Garzanti *et al.* 1995) with a bimodal felsic–mafic volcanism marked by effusion of olivine basalts and rhyolitic ignimbrites, probably marking transition to a continental-rifting stage in intra-arc settings (Garzanti *et al.* 2003). This arc-related Mid-Triassic volcanic activity lasted between Late Anisian (top of the Prezzo Formation) and Late Carnian (top

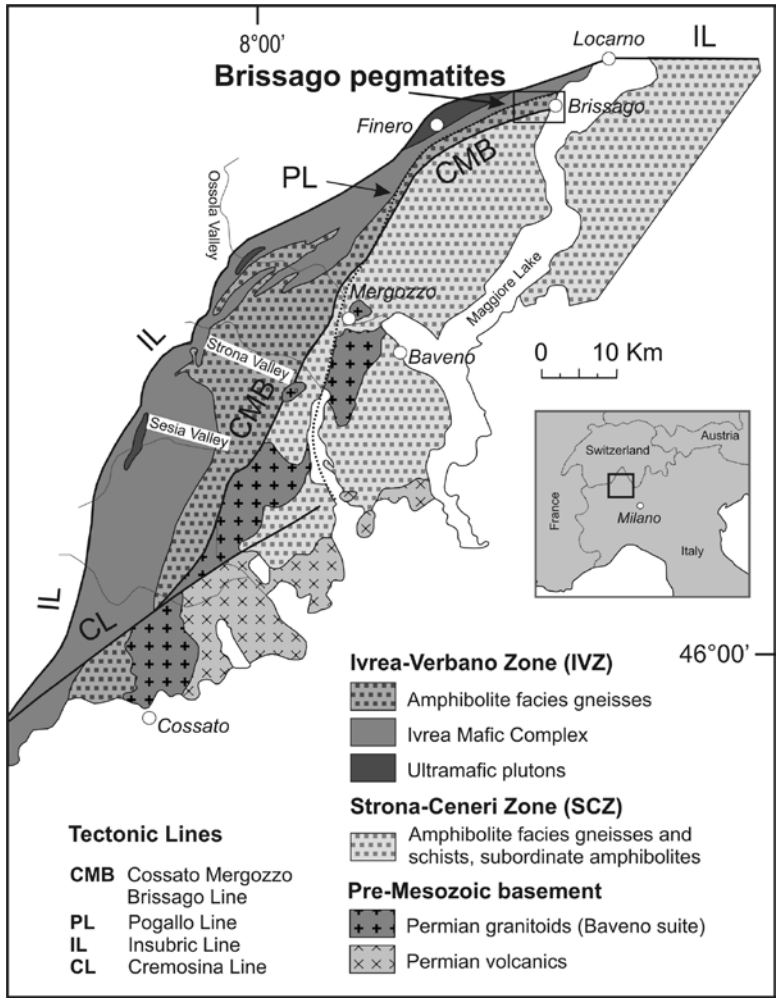

FIG. 1. Regional geology of Ivrea–Verbano and Strona–Ceneri zones (South Alpine basement), and the position of Brissago granitic pegmatites (modified after Mulch *et al*. 2002).

of the San Giovanni Bianco Formation, Gaetani *et al*. 1998). The initial and terminal stages of volcanism have been accurately dated geochronologically as 241 Ma (Anisian–Ladinian boundary; Mundil *et al*. 1996) and 231 Ma (Late Carnian; Furin *et al*. 2006).

The third tectono-magmatic cycle lasted from Norian to Liassic times (225–185 Ma) when the South Alpine continental crust was involved in rifting, which led to formation of the Adriatic passive margin in the Middle Jurassic (Bertotti *et al*. 1999, Jadoul *et al*. 1992). Late Triassic to Early Jurassic extensional tectonics led to the uplift of subcontinental mantle, evidenced by a reheating event at 215±15 Ma (Lu *et al*. 1997) and K and Na metasomatism of the Finero Complex at 207 Ma with the emplacement of zircon-bearing pegmatites within the Finero ultrabasic complex and country rocks (Grieco *et al*. 2001, Oppizzi & Schaltegger 1999).

Geology of the Ivrea–Verbano Zone

The Brissago granitic pegmatites are emplaced into the Kinzigitic Complex of the Ivrea–Verbano Zone (IVZ), a suite of Paleozoic high-grade metamorphic rocks inferred to represent a portion of deep continental crust (Giese 1968, Fountain 1976) (Fig.1). The Ivrea–Verbano Zone is separated from the Alps *sensu stricto* by the Insubric Line (Heitzmann 1987, Schmid *et al*. 1987, Zingg & Hunziker 1990) and from the Serie dei

Laghi (Strona–Ceneri Zone) by the Pogallo and the Cossato–Mergozzo–Brissago lines (Handy 1986, 1987, Boriani & Sacchi 1973, Boriani *et al*. 1990).

The Kinzigitic complex, which together with the Mafic Formation ("Basischer Hauptzug" auct.) constitutes the Ivrea–Verbano Zone, is made up of upper-amphibolite-facies metapelites (kinzigites *sensu stricto*) (see Walter 1950 for more details), granulite-facies metapelites ("stronalites"), amphibolites and marbles. The Brissago granitic pegmatites were found along Valle di Ponte from the Lago Maggiore shore westward to the Gridone watershed. Field work points to the presence of E–W-oriented and subvertical dikes of hornblende diorite, granite, aplite and granitic pegmatite containing muscovite, garnet, schorl, zircon, beryl and Fe–Cu sulfides, but lacking phosphates. Coarse-grained pegmatitic boulders, containing phosphate masses, were encountered only in the lower part of Valle di Ponte.

The Phosphate-Bearing Pegmatites

As described by previous investigators (De Quervain 1932, Walter 1950), several small boulders of coarse-grained granitic pegmatite containing phosphates masses were encountered only in the lower part of Valle di Ponte in two elongated accumulations oriented E–W. These accumulations probably are the result of the *in situ* break-up of pegmatite dikes due to geomorphological agents. We speculate that the original pegmatite dikes were oriented E–W with a subvertical dip. In the same restricted area, in 1999, the phosphate-bearing pegmatite boulder described in this work was found, and named "ZPU" according to its significant contents of zircon, phosphates and uraninite.

The samples studied were collected from the "ZPU" boulder. The boulder, found in slope wash at an elevation of 420 m above sea level and measuring 1 × 1.5 × 0.8 meters, shows the whole cross-section of the dike. The contact with the enclosing amphibolite, still present on one side of the boulder, looks sharp. The dike has an asymmetrical zonal structure composed of four main units: 1) aplite unit, 2) plagioclase + quartz graphic unit containing schorl, 3) coarse-grained plagioclase unit (albite) with minor K-feldspar, and 4) quartz core with muscovite, garnet and accessories (Fig. 2). The pegmatite has an overall "granitic" composition given by albite, quartz ± muscovite. The phosphate masses are embedded into the quartz core unit or between the core unit and the plagioclase + quartz graphic unit. Two types of phosphate masses are present in the ZPU boulder: graftonite–triphylite masses containing the related hydrothermal products, and F-rich manganoan apatite-(CaOH) in monomineralic masses. Commonly, the graftonite–triphylite masses are rimmed by a layer of garnet crystals, whereas vivianite and Fe–Mn-oxides form thin impregnations along the contact with the hosting pegmatite. Locally, at the rim of the graftonite–triphylite masses, euhedral crystals of F-rich apatite-(CaOH) were found. Tiny grains (5–10 μm in size) of U- and Th-rich monazite-(Ce) were found disseminated in the phosphate masses. Other common accessories found in the ZPU boulder are garnet, zircon, uraninite, columbite-(Fe) and secondary minerals of uranium (Weiss *et al*. 2004).

The samples collected from the ZPU boulder and used for this study are deposited at the "Museo Cantonale di Storia Naturale", Lugano, Canton Ticino, Switzerland.

Analytical Methods

Besides accurate textural observations, 23 samples (Table 1) were examined using a Cambridge Stereoscan 250 electron microscope equipped with an Oxford Link AN 10000 energy-dispersive spectrometer, then analyzed using an Applied Research Laboratories electron microprobe fitted with six wavelength-dispersive spectrometers and a Tracor Northern energy-dispersive spectrometer at the CNR – Istituto per la dinamica dei processi ambientali laboratories in Milano. The back-scattered electron images were acquired at a working distance of 25 mm and an accelerating voltage of 20 kV, and quantitative WDS analyses were made at 15 kV accelerating voltage and 300 nA beam current. A series of minerals (kaersutite for Mg, Si, Fe, Al, Na, K, rhodonite for Mn, apatite for P, Ca and F, sodalite for Cl) were used as standards. The results were processed for matrix effects by a conventional ZAF routine of the Tracor Northern Task package. Selected results of analyses are reported in Tables 2, 3, 4 and 5.

Moreover, *in situ* U–Pb geochronology was carried out by excimer laser ablation (ELA)–ICP–MS at the C.N.R. – Istituto di Geoscienze e Georisorse U.O. di Pavia. The instrument couples a 193 nm excimer laser microprobe (Compex 102 from MicroLas) with a sector-field ICP–MS (Element-I from ThermoFischer). Details of the analytical method are reported in Tiepolo (2003). The laser was operated at 5 Hz, the spot size was set to 20 μm, and the laser fluence to 12 J/cm^2. Instrumental mass bias and laser-induced elemental fractionation are corrected with the adoption of zircon 91500 (Widenbeck *et al*. 1999) as external matrix-matched standard. Data reduction was carried out using the "Glitter" software package (van Achterbergh *et al*. 2001). The same integration intervals were used on the standard and unknown samples, and the reproducibility on the standards was propagated to all determinations according to the equation in Horstwood *et al*. (2003). The Isoplot/Ex 3.0 software (Ludwig 2000) was used to calculate concordia ages and draw concordia plots.

Results

Careful observation of all hand samples collected from the ZPU allowed us to highlight the presence of two different associations of phosphates within the

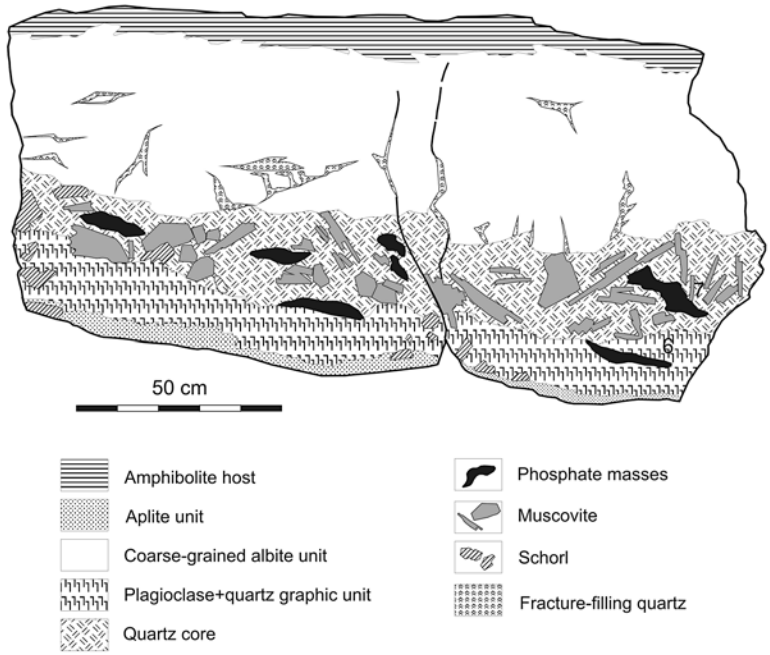

FIG. 2. Cross section of the ZPU boulder showng the pegmatite zones and the position of the phosphate masses.

graftonite–triphylite masses. Association I is characterized by an evident lamellar texture and medium to dark brown color. Association II is characterized by a microgranular aspect with color ranging from pale pink to greenish grey. Garnet, chamosite and plagioclase were found closely associated with the phosphates.

Association I

At Brissago, intergrowths of phosphates with a marked lamellar texture are very rare and characterize very small parts of the core of the phosphate masses. Observations made on hand specimens and thin sections point out a gradual transition from a lamellar to a polygonal texture. For instance, sample BRI 10B contains triphylite lamellae (from 5 to 10 μm thick and from 100 to 600 μm long) embedded in graftonite and in direct contact with some triphylite micrograins (Fig. 3A). In the core of the phosphate mass ZPU 76, a very small portion, up to 3 mm, with lamellar texture was found. The intergrowth shows a groundmass constituted by coarse, rounded crystals of graftonite hosting platy lamellae of triphylite (Figs. 3B, 4A, B). The optical orientation of triphylite, where still present, is largely uniform over the whole analyzed specimen. In this association, triphylite appears deeply altered to a pale-honey yellow color (Fig. 4B), and it is commonly replaced by brown ferrisicklerite and heterosite following the Quensel–Mason sequence (Quensel 1937, Mason 1941). Almost complete gradual transitions between triphylite and ferrisicklerite and between ferrisicklerite and heterosite are commonly observed within the lamellae. Heterosite forms irregular masses hosted in graftonite, probably as an oxidation product of triphylite granules. Rare irregular grains of staněkite from 10 to 50 μm in size are hosted in graftonite. This secondary phosphate, typical of hydrothermally oxidized associations (Roda *et al*. 2004), is partially replaced by heterosite (Fig. 3B). Exceptionally, some elliptical grains of kryzhanovskite up to 50–100 μm in size and showing a perfect cleavage were found embedded in heterosite replacing triphylite lamellae. It probably represents an oxidation product of ferrisicklerite, as described for the kryzhanovskite found at Okatjimukuju farm pegmatites by Keller & von Knorring (1989). In all analyzed samples, graftonite belonging to association I shows low contents of Mn (12.89–13.41 wt% MnO), high contents of Ca (10.79–12.87 wt% CaO) and Mg (2.12–3.80 wt% MgO), and its Fe/(Fe + Mn) value ranges from 0.69 to 0.71 (Table 2). The chemical composition of triphylite is very close to that of the end-member. It contains 6.76–8.34 wt% MgO, and has a Fe/(Fe + Mn) value ranging from 0.88 to 0.90 (Table 2). Oxidized products of triphylite characterize the association of secondary

phosphates in lamellar aggregates. Ferrisicklerite, formed after Li leaching and partial oxidation of Fe in triphylite (Mason 1941, Moore 1973, Fransolet *et al.* 1985, 1986), shows a remarkably high Mg content (8.22 wt% MgO), low content of Mn (3.13 wt% MnO) with Fe/(Fe + Mn) value of 0.90, close to that of the parent triphylite (Table 3). High Mg values were described for ferrisicklerite found in the border-zone phosphate

TABLE 1. DESCRIPTION OF ANALYZED SAMPLES, BRISSAGO GRANITIC PEGMATITE

Microprobe sample		Reference sample	Description of microprobe sample and local position	Assemblage of minerals	BSE aspect
BRI 1		ZPU 11–GL1b	Contact between mass of "phosphates" and quartz core	jahnsite-(CaMnFe) mitridatite apatite-(CaOH)	replacing Gft microscopic groundmass
BRI 2		ZPU 11–GL1b	I) Brownish-pink "phosphate" with transparent zones, II) earthy dark yellow "phosphate" at the contact with quartz. Contact is outlined by III) a rim of garnet crystals	jahnsite-(CaMnFe)	replacing Gft
BRI 3		ZPU 11–GL1b	Rose-grey "phosphate" mass with a yellow-green rim	jahnsite-(CaMnFe) ludlamite apatite-(CaOH)	replaces Gft microscopic groundmass
BRI 4	A	ZPU 3–GL3	Transparent salmon pink or orange "phosphate"	graftonite	groundmass
	B	ZPU 7–GL 7	Transparent brownish pink or greenish grey "phosphate"	graftonite triphylite ludlamite	groundmass microscopic microscopic
	C	ZPU–GL12 a+b	Transparent salmon pink "phosphate"	graftonite jahnsite-(CaMnMn) triphylite	groundmass microscopic microscopic
BRI 6		ZPU 11–GL1b	Prismatic, transparent olive oil yellow crystal of apatite at the rim of a "phosphate" mass"	apatite-(CaOH)	
BRI 7	A	ZPU 81–GL 12 a/b	Yellowish grey, dull mass of apatite mass	(a) apatite-(CaOH) (b) almandine	
	B	ZPU 75–GL 1b	Vivianite, small mass mixed with quartz	vivianite	
BRI 9	A	ZPU 75–GL 1b	"Phosphate" rim garnet	almandine	
	B	ZPU 81–GL 12 a/b	Garnet: quartz core associated with muscovite and zircon	(c) almandine	
	C	ZPU 63–GL 9b	Garnet : host-rock contact,	almandine	
	D		quartz core near "phosphate"	almandine	
	F		mass	(d) almandine, chamosite	
	E	ZPU 63–GL 9b	Endocontact plagioclase	(e) plagioclase 15 mol.% An	
BRI 10	A	ZPU 75–GL 1b	A: "phosphate": transparent salmon pink portion at the center of the mass	jahnsite-(CaMnFe) ludlamite	groundmass microscopic
	B		B: "Phosphate": transparent pink portion at the rim of mass	graftonite triphylite ludlamite maghagendorfite	groundmass microscopic and lamellae microscopic microscopic
	C		C: "Phosphate": pink portion of a mass with milky stripes	jahnsite-(CaMnFe) ludlamite	groundmass microscopic
TS		ZPU 79	Contact between quartz core and coarse-grained albite unit	almandine (a), albite 99 mol.% (f), muscovite	
TS		ZPU 76	Graftonite with triphylite lamellae almost completely replaced by ferrisicklerite and heterosite at the core of a microgranular mass of phosphate	graftonite triphylite ferrisicklerite heterosite kryzhanovskite stanĕkite	groundmass lamellae replaces Trp replaces Trp grains grains

Symbols: Gft: graftonite, Trp: triphylite. TS: thin section.

TABLE 2. SELECTED ELECTRON-MICROPROBE DATA ON THE PRIMARY PHOSPHATES

	graftonite						triphylite					maghagen-dorfite
	monocrystalline masses (magmatic)			micrograins (metamorphic)			lamellae (magmatic)			micrograins (metamorphic)		
	BRI 10B	ZPU 76 TS	ZPU 76 TS	BRI 4A (a,c)	BRI 4B (b,c)	BRI 4C (a,b)	ZPU 76 TS	ZPU 76 TS	ZPU 76 TS	BRI 4B	BRI 4C (b)	BRI 10B
N	3	3	3	8	6	3	3	3	3	3	4	2
P_2O_5 wt%	41.36	42.69	42.40	42.61	41.72	42.03	47.30	47.63	47.69	49.69	49.17	43.79
SiO_2	—	—	—	0.15	0.09	0.06	—	—	—	0.13	0.05	—
MgO	2.12	2.80	2.14	3.02	2.09	2.08	6.76	8.34	7.91	9.11	8.68	9.21
CaO	11.30	10.79	12.87	10.63	12.54	12.25	1.53	0.30	0.19	0.07	0.28	5.49
MnO	13.41	12.89	12.97	11.29	11.94	10.84	4.00	3.41	3.56	2.98	2.74	9.43
FeO	32.16	31.65	29.91	31.37	29.65	30.20	30.18	30.04	30.62	29.53	29.20	28.07
Na_2O	0.01	0.20	0.24	—	—	—	0.13	0.15	—	—	—	5.66
Li_2O‡	----	----	----	----	----	----	9.99	10.07	10.06	10.23	10.24	----
sum	100.36	101.02	100.52	99.06	98.02	97.45	99.89	99.93	100.02	101.75	100.34	101.65
P *apfu*	1.986	2.012	2.009	2.030	2.019	2.037	0.997	0.996	0.998	1.006	1.011	2.981
Si	----	----	----	0.008	0.005	0.003	----	----	----	0.003	0.001	----
Mg	0.179	0.232	0.178	0.253	0.178	0.177	0.251	0.307	0.292	0.325	0.314	1.104
Ca	0.687	0.644	0.772	0.641	0.768	0.752	0.041	0.008	0.005	0.002	0.007	0.473
Mn^{2+}	0.644	0.608	0.615	0.538	0.578	0.526	0.084	0.071	0.075	0.060	0.056	0.642
Fe^{2+}	1.525	1.474	1.400	1.476	1.417	1.446	0.628	0.620	0.633	0.591	0.593	1.888
Na	0.001	0.022	0.026	----	----	----	0.006	0.007	----	----	----	0.883
Li	—	—	—	—	—	—	1.000	1.000	1.000	1.000	1.000	—
Σ *M*	3.035	2.980	2.991	2.909	2.942	2.900	2.011	2.014	2.004	1.978	1.971	4.989
Fe#	0.70	0.71	0.69	0.73	0.71	0.73	0.88	0.90	0.89	0.91	0.91	0.75

Notes: a) Cl, traces below detection limit; b) K, traces below detection limit; c) Ti, traces below detection limit. ‡ calculated for 1 lithium atom in stoichiometry; N = number of averaged points of analysis. The structural formulae of the minerals are calculated on the basis of a fixed number of atoms of oxygen per formula unit (*apfu*), as follows: graftonite: 8, triphylite: 4, maghagendorfite: 12.

association of the Cañada granitic pegmatite (Roda *et al*. 2004). Heterosite has the same chemical characters of ferrisicklerite with a Fe/(Fe + Mn) value ranging between 0.86 and 0.90 (Table 3). Krizhanovskite shows an appreciable amount of Mg (4.45 wt% MgO), with a Fe/(Fe + Mn) value of 0.79 (Table 3). Staněkite shows a chemical composition close to that described by Roda *et al*. (2004), with a Fe/(Fe + Mn) value of 0.71; it represents the second occurrence in the Alps (Guastoni *et al*. 2007).

Association II

The study of thin sections points out a widespread seriate–polygonal to seriate–interlobate medium- to fine-grained texture of the main phosphate mass. Micrograins are observed whether as fillings along grain contacts or scattered into the main mass of phosphate; they give a pseudopoikilitic texture to the assemblage (Fig. 4C). The examination of more than 100 back-scattered electron images indicates a great number of micrograins (from 50 to 100 μm in size) differing in chemical composition from the groundmass (Figs. 3C, D). The microgranules do not show a preferential orientation or concentration, but are spread and randomly oriented into the groundmass. As can be inferred from back-scattered electron images combined with chemical data, the mineralogical association of primary phosphates in these masses is dominated by graftonite followed by triphylite micrograins, of the order of 5 vol.%. Maghagendorfite is present in very small amounts. Jahnsite-(CaMnFe) is the most abundant secondary phosphate, followed by vivianite, ludlamite, jahnsite-(CaMnMn) and mitridatite. The amount of secondary phosphates approaches 1–2% of the total phosphate association and mostly appears at the rim of microgranular phosphate masses. Vivianite mainly constitutes impregnations along grains boundaries and rarely is found as a replacement of the main phosphate mass, where pale green ludlamite replaces triphylite grains. Jahnsite-(CaMnMn) and mitridatite are very rare at Brissago and never show well-defined grains, but rather give gradual transitions due, respectively, to Mn and Ca increase in the hosting jahnsite-(CaMnFe)

TABLE 3. SELECTED ELECTRON-MICROPROBE DATA ON HYDROTHERMAL PHOSPHATES

	association I					association II									
	ferri-sicklerite	hetero site		kryzha-novskite	staněk-ite	jahnsite					mitridatite		ludlamite		vivianite
	ZPU 76	ZPU 76	ZPU 76	ZPU 76	ZPU 76	BRI 1-I	BRI 2-I	BRI 4C	BRI 10C	BRI 10A	BRI 1-II	BRI 3-1	BRI 4-B	BRI 10A-C	BRI 7
N	3	3	3	3	3	5	9	2	2	1	1	1	2	2	3
P_2O_5 wt%	46.05	50.75	48.49	36.57	33.31	34.98	35.30	36.22	37.72	35.73	36.89	37.99	32.25	33.48	29.75
SiO_2	—	—	—	—	—	0.14	0.02	0.02	—	—	0.09	—	0.03	0.09	—
Mn_2O_3	—	3.96	6.03	—	—	—	—	—	—	—	9.85	10.41	—	—	—
Fe_2O_3	†30.84	†34.66	†35.6	†36.97	‡36.75	*19.2	*19.48	*19.59	*20.43	*19.45	†26.65	†24.34	—	—	—
MgO	8.22	8.91	6.96	4.45	2.28	0.94	2.38	2.12	2.17	2.25	0.36	1.19	11.29	12.94	—
CaO	0.63	0.38	0.40	1.12	0.32	6.70	8.88	8.37	9.51	10.06	17.67	17.39	0.15	0.11	0.17
MnO	3.13	—	—	9.93	18.21	8.59	9.35	8.85	10.21	9.57	—	—	3.52	2.79	5.43
FeO	—	—	—	—	7.60	13.14	8.22	8.23	6.81	5.52	—	—	35.75	34.89	39.58
Na_2O	0.19	0.24	—	0.24	0.35	—	—	—	—	—	—	—	—	0.13	—
Li_2O	°10.54	—	—	—	—	—	—	—	—	—	—	—	—	—	—
sum	99.60	98.89	97.48	89.28	98.82	83.70	83.63	83.40	86.85	82.58	91.51	91.32	82.99	84.43	74.93
P *apfu*	0.919	1.039	1.021	2.048	1.019	4.098	4.077	4.160	4.155	4.133	3.144	3.212	1.848	1.857	1.998
Si	—	—	—	—	—	0.019	0.003	0.003	—	—	0.009	—	0.002	0.006	—
Mn^{3+}	—	0.072	0.113	—	—	—	—	—	—	—	0.755	0.791	—	—	—
Fe^{3+}	0.547	0.631	0.666	1.840	1.000	2.000	2.000	2.000	2.000	2.000	2.019	1.830	—	—	—
Mg	0.289	0.321	0.258	0.439	0.123	0.194	0.484	0.429	0.421	0.458	0.054	0.177	1.139	1.264	—
Ca	0.016	0.010	0.011	0.079	0.013	0.994	1.298	1.217	1.326	1.473	1.906	1.861	0.011	0.008	0.014
Mn^{2+}	0.062	—	—	0.556	0.558	1.007	1.080	1.017	1.125	1.107	—	—	0.202	0.155	0.365
Fe^{2+}	—	—	—	—	0.230	1.521	0.938	0.934	0.741	0.631	—	—	2.024	1.912	2.626
Na	0.009	0.011	—	0.031	0.025	—	—	—	—	—	—	—	—	0.017	—
Li	1.000	—	—	—	—	—	—	—	—	—	—	—	—	—	—
Σ *M*	1.923	1.045	1.048	2.945	1.947	5.716	5.800	5.596	5.613	5.669	4.734	4.659	3.376	3.354	3.005
Fe#	0.90	0.90	0.86	0.79	0.71	0.78	0.73	0.74	0.71	0.70	0.73	0.70	0.91	0.93	0.88

Notes: N = number of averaged points of analysis; ° calculated for 1 Li^{1+} atoms in stoichiometry; † total Fe calculated as Fe_2O_3; ‡ calculated for 1 Fe^{3+} atoms in stoichiometry; * calculated for 2 Fe^{3+} atoms in stoichiometry. Fe# = $Fe_{tot}/(Fe_{tot} + Mn_{tot})$. The structural formulae of the minerals are calculated on the basis of a fixed number of atoms of oxygen per formula unit (*apfu*), as follows: ferrisicklerite and heterosite: 4, kryzhanovskite: 9, staněkite: 5, jahnsite: 17, mitridatite: 14, ludlamite and vivianite: 8.

groundmass in close association with manganoan apatite-(CaOH). Graftonite and triphylite belonging to association II show chemical features very close to those of the same minerals in association I (Table 2). In particular, graftonite has low contents of Mn (10.84–11.94 wt% MnO), high contents of Ca (10.63–12.54 wt% CaO) and Mg (2.08–3.02 wt% MgO), and its Fe/(Fe + Mn) value ranges from 0.71 to 0.73 (Table 2). Triphylite granules contain 6.86–9.11 wt% MgO, and have a Fe/(Fe + Mn) value of 0.91. Grains (20–100 μm, Fig. 3D) of a Mg-, Na- and Ca-bearing iron phosphate belonging to the alluaudite group rarely occur in the polycrystalline phosphate mass (*e.g.*, ZPU 75, sample BRI 10B; Tables 1, 2). The unusual pale brown grains are hosted in graftonite and associated with ludlamite (Fig. 3D). Chemical analyses of this phosphate reveal an excess of Fe, Mg and Ca and a strong deficit in Mn, with respect to the data proposed for maghagendorfite from Dyke Load, Custer, South Dakota by Moore & Ito (1979) and by Fleischer *et al.* (1980). Nevertheless, following the general structural formula proposed by Moore (1971) and modified by Hatert *et al.* (2000) for the alluaudite group, $X(2)X(1)M(1)M(2)_2(PO_4)_3$, the crystal-chemical formula for the maghagendorfite found at Brissago can be written as: $(Mg^{2+})_{\Sigma 1}(Na^{1+}_{0.88}Ca^{2+}_{0.12})_{\Sigma 1}(Mn^{2+}_{0.64}Ca^{2+}_{0.35})_{\Sigma 0.99}(Fe^{2+}_{1.89}Mg^{2+}_{0.10})_{\Sigma 1.994}(P^{5+}_{2.98}O^{2-}_{12})$, with a charge balance of –0.02. Maghagendorfite grains found at Brissago show sharp contacts with the hosting graftonite without any sign of replacement or alteration (Fig. 3D). Moreover, petrographic relationships illustrate that graftonite and maghagendorfite crystallized together. These characteristics, described for primary hagendorfite from the Kibingo granitic pegmatite by Fransolet

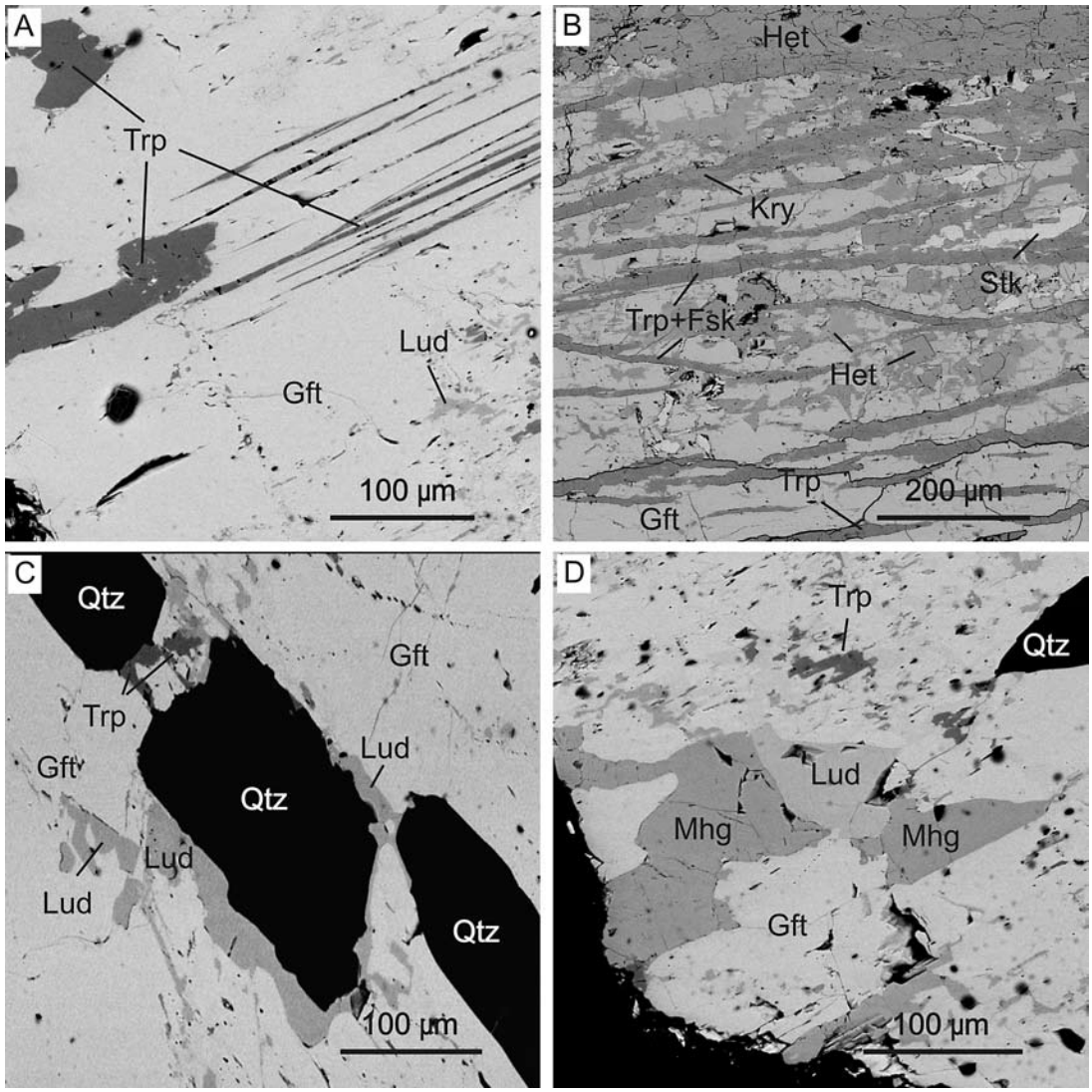

FIG. 3. Back-scattered electron (BSE) images of Brissago phosphate masses. A) Sample BRI 10–B, graftonite groundmass (Gft) with triphylite lamellae and grains (Trp), and microgranules of ludlamite (Lud). B) Sample ZPU 76 (thin section), graftonite groundmass (Gft) with triphylite lamellae (Trp) partially or totally replaced by ferrisicklerite (Fsk) and heterosite (Het) associated to (Stk) and kryzhanovskite (Kry). C) Sample BRI 10–B, graftonite groundmass (Gft) with microgranules of triphylite (Trp) and ludlamite (Lud) rimming quartz grains (Qtz). D) Sample BRI 10–B, graftonite groundmass (Gft) with microgranules of maghagendorfite (Mhg), triphylite (Trp), and ludlamite (Lud).

et al. (2004), lead us to consider maghagendorfite as a primary phosphate in the Brissago granitic pegmatites. Jahnsite-(CaMnFe) is the most abundant hydrothermal phosphate found at the rim of polycrystalline masses, in close association with apatite-(CaOH). It replaces graftonite, forming very localized and fine polycrystalline aggregates absent at the rim of phosphate masses. The chemical composition of the jahnsite (Table 3) is rather variable, between jahnsite-(CaMnFe) and jahnsite-(CaMnMn): the first one shows an excess of Fe with respect to the stoichiometry (*e.g*., BRI 1–I, Table 3), whereas the second one is higher in Ca and lower in Fe (*e.g*., BRI 10–A, Table 3). This trend is characterized by an increase of Mg (0.94–2.38 wt% MgO) and Mn (9.85–10.41 wt% MnO) and by a decrease in Fe/(Fe + Mn) from 0.78 to 0.7. Mitridatite, closely asso-

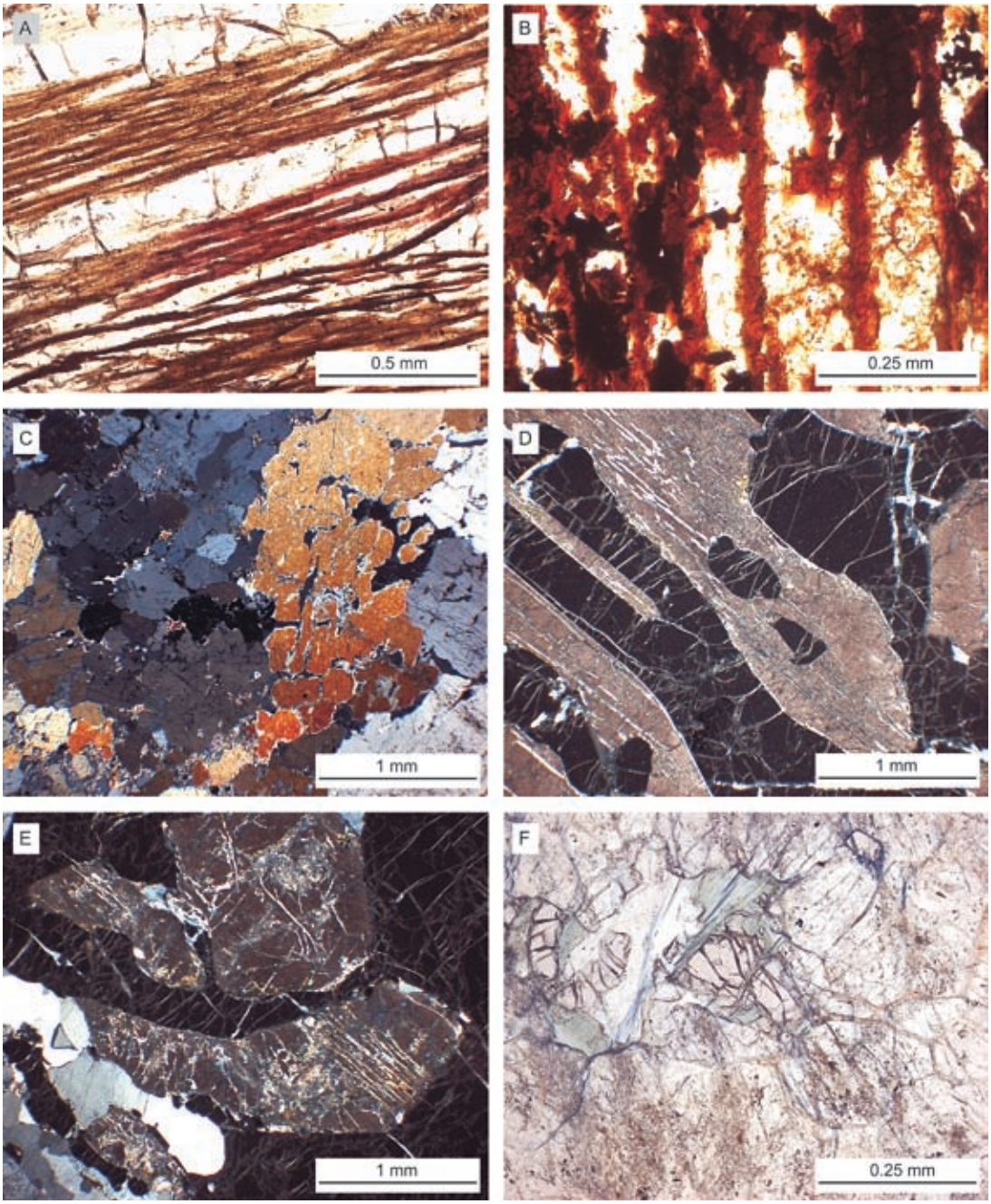

FIG. 4. Polarizing microscope images: A) white graftonite groundmass with triphylite lamellae replaced by brown ferrisicklerite and reddish brown heterosite (sample ZPU 76, plane-polarized light). B) White graftonite groundmass with triphylite lamellae partially or totally replaced by pale brown ferrisicklerite and reddish brown heterosite associated to dark brown to opaque grains of staněkite (sample ZPU 76, plane-polarized light). C) Polycrystalline mass of graftonite (sample ZPU 75, crossed nicols). D and E) Graftonite masses with triphylite lamellae corroding huge crystals of garnet (sample ZPU 74, crossed nicol). F) Pale pink fractured relics of garnet hosted by polycrystalline graftonite and associated to clinochlore (sample ZPU 76, plane-polarized light).

ciated with jahnsite and apatite, shows a high content of Mn and a Fe/(Fe + Mn) value of 0.7. Ludlamite is found only as micrograins hosted by graftonite, mainly at the rim of the phosphate masses (Figs. 3A, C, D). The chemical data for vivianite show an appreciable content of Mn (5.97 wt% MnO) (Table 3). The Fe/(Fe + Mn) value of ludlamite and vivianite ranges from 0.88 to 0.93; these values are close to those of triphylite (Table 2).

Both massive and euhedral apatite-(CaOH) have a similar composition, with a high F content; Mn also is present, with a concentration ranging from 4.02 to 4.47 wt% MnO, a common occurrence in granitic pegmatites (Table 4). The massive primary apatite-(CaOH) can be distinguished from the euhedral secondary apatite-(CaOH) only on the basis of morphological characteristics (Moore 1973).

The associated silicates

Garnet appears as a rim or directly embedded in phosphate masses. In the first case, the subhedral crystals of garnet are deeply indented by phosphates (Figs. 4D, E). In the second case, garnet is found as anhedral relics hosted by phosphates (Fig. 4F). In both cases, garnet is deeply fractured and partially replaced by chamosite, mainly along fractures. The chemical composition is almost constant, corresponding to almandine with a substantial proportion of the spessartine components and a much smaller amount of the pyrope component. Its Fe/(Fe + Mn) value ranges between 0.71 and 0.72 (Table 5). Plagioclase shows rather constant compositions near 100% Ab along all dike section; oligoclase compositions (An_{15}) were detected only within the endocontact of the dike (Tables 1, 5).

Age determination

Two zircon grains (Z1C1 and Z1C2) up to 2.0 × 1.2 mm in size were sampled from the ZPU boulder. Prior to the *in situ* ELA–ICP–MS analyses of the zircon, the internal structure was investigated by cathodoluminescence (CL) and with back-scattered electron (BSE) images. Both zircon grains show a core rich in inclusions and characterized by extensive recrystallization, but the outer boundaries are homogeneous and with very low CL emission. The *in situ* geochronological approach allowed us to analyze only the preserved rims of zircon; we avoided the altered cores. Sixteen analyses were carried out on these external rims and most data (11 spots) yield concordant results (Table 6). Nine analyses cluster between 238 ± 4.7 and 248.6 ± 4.9 Ma (2σ) and define a mean concordia age of 242.3 ± 2.8 Ma (95% confidence), which is inferred to represent the age of crystallization of the zircon (Fig. 5). Two analyses yield significantly younger ages, 219.5 ± 9.9 and 229 ± 10 Ma (2σ) that likely represent a postmagmatic resetting of the U–Pb system.

TABLE 4. SELECTED ELECTRON-MICROPROBE DATA ON APATITE-(CaOH)

N	primary BRI 7A 4	hydrothermal BRI 6 4		primary BRI 7A	hydrothermal BRI 6
P_2O_5 wt%	41.57	41.99	P *apfu*	3.068	3.083
CaO	49.34	49.90	Ca	4.609	4.637
MnO	4.47	4.02	Mn^{2+}	0.330	0.295
FeO	2.25	2.03	Fe^{2+}	0.164	0.147
Cl	0.84	0.93	Σ *M*	5.103	5.079
F	1.53	1.60			
-O=F,Cl	-0.83	-0.88	Cl	0.062	0.068
			F	0.211	0.219
sum	99.16	99.59			
			Fe#	0.33	0.34

The formula of apatite-(CaOH) is calculated on the basis of 12.5 atoms of oxygen per formula unit (*apfu*). Fe# = $Fe_{tot}/(Fe_{tot} + Mn_{tot})$. N: number of averaged points of analysis.

DISCUSSION OF THE DATA

The association of secondary minerals, especially the presence of a conspicuous amount of phosphates, together with columbite-group minerals, indicates that

TABLE 5. SELECTED ELECTRON-MICROPROBE DATA ON GARNET AND PLAGIOCLASE

	garnet				plagioclase	
	(a) ZPU 79 TS	(b) BRI 7A	(c) BRI 9 B II	(d) BRI 9F	(e) BRI 9E	(f) ZPU 79 TS
N	4	8	4	4	4	10
SiO_2 wt%	35.92	36.17	36.08	36.82	67.29	68.39
TiO_2	0.02	0.01	0.01	0.01	0.33	0.01
Al_2O_3	20.77	21.46	21.20	21.37	22.47	20.38
Fe_2O_3	1.86	1.36	1.42	1.19	---	---
FeO	30.04	30.38	30.43	30.45	0.03	0.03
MnO	10.34	10.43	10.14	10.44	0.01	0.01
MgO	1.13	1.07	1.11	1.41	0.03	0.01
CaO	0.32	0.28	0.33	0.35	2.38	0.21
Na_2O	0.00	0.01	0.01	0.02	7.33	10.79
K_2O	0.01	---	---	---	0.00	0.05
sum	100.41	101.17	100.73	102.06	99.86	99.86
Si *apfu*	2.940	2.933	2.939	2.954	3.035	3.008
Ti	0.001	0.001	0.001	0.001	0.011	---
Al	2.004	2.051	2.035	2.021	1.194	1.057
Fe^{3+}	0.115	0.083	0.087	0.072	---	---
Fe^{2+}	2.056	2.061	2.073	2.043	0.001	0.001
Mn^{2+}	0.717	0.716	0.700	0.709	---	---
Mg	0.001	0.001	0.001	0.001	0.002	0.001
Ca	0.028	0.024	0.029	0.030	0.115	0.010
Na	---	0.002	0.002	0.002	0.641	0.920
K	0.001	---	---	---	---	0.003
Alm mol.%	70	70	71	69		
Sps	24	24	24	24		
Prp	5	4	5	6		
Ab					85	99
An					15	1
$Fe_{tot}/(Fe_{tot}+Mn_{tot})$	0.71	0.72	0.72	0.72		

Notes: (a) rim of "phosphate" mass, (b) rim of "phosphate" mass, (c) core-blocky feldspar contact near a "phosphate" mass, (e) contact with the amphibolite host, (f) coarse-grained albite unit at the contact with quartz core. N: number of averaged points of analysis. TS: thin section. The formulae of almandine and plagioclase are calculated on the basis of 12 and 8 atoms of oxygen per formula unit (*apfu*).

these pegmatites belong to the rare-element LCT family in the classification of Černý & Ercit (2005).

Degree of evolution of the pegmatite-forming melt

At Brissago, the chemical composition of primary phosphates and associated garnet is clearly Fe-dominant, with high Ca and Mg contents in graftonite and a high Mg content in triphylite. High Ca and fairly high Mg contents in graftonite are described in graftonite–triphylite intergrowths from Nåttarö and Stora Persholmen pegmatites in Sweden by Smeds *et al.* (1998) and from the Conifer Road pegmatite in northwestern Ontario by Černý *et al.* (1998). Roda *et al.* (2004) reported high Ca contents in graftonite found in the phosphate association belonging to the border zone of the Cañada pegmatite in eastern Spain. Triphylite with a high Mg content was found associated with graftonite in lamellar intergrowths from the Bötsudden and Rånö pegmatites (Smeds *et al.* 1998). Such chemical features for graftonite and triphylite are typical of poorly evolved LCT granitic pegmatites (Smeds *et al.* 1998, Černý *et al.* 1998) or of less-evolved facies of evolved Li–P-bearing pegmatites (Roda *et al.* 2004).

The prominence of Fe over Mn in primary phosphates and garnet, which represents the most widespread mafic phase after phosphates, the high Ca and Mg contents in graftonite and triphylite, respectively, and the predominance of graftonite over triphylite indicate that at Brissago, the phosphate-bearing pegmatites are poorly fractionated and geochemically primitive.

Mechanisms of crystallization

According to many authors (Hurlbut 1965, Wise & Černý 1990, Smeds *et al.* 1998, Černý *et al.* 1998), the textural features and optical characteristics point to graftonite–triphylite lamellar intergrowths of association I as having crystallized at the magmatic stage. They can be considered an exsolution product of a high-temperature Ca-rich and, to a lesser extent, Mg- and Li-rich, disordered, graftonite-like parent phase. A later decrease in temperature caused the migration of Ca in graftonite and of Mg and Li into triphylite, which has an olivine-type structure (Moore 1973). The presence, even if a small amount, of Li in the parent phosphate favored the exsolution of triphylite instead of sarcopside (Hurlbut 1965). At the same stage, the high concentration of Ca and $[PO_4]^{3-}$ allowed the crystallization of masses of primary apatite-(CaOH). Following the experimental work of London *et al.* (1999), the Fe/(Fe + Mn) value of graftonite (ranging from 0.70 to 0.73) and of garnet (ranging from 0.68 to 0.72) in contact with phosphate masses may indicate that the phosphate originated as a result of phosphorus-induced destabilization of garnet (Figs. 4D, E, F). In this case, the increase in concentration of phosphorus in the melt induced the destabilization of the previously formed garnet, and the development of the high-temperature graftonite-like parent phase and of masses of primary apatite. Hydrothermal products of oxidation of the Quensel–Mason sequence are well represented within association I, in which ferrisicklerite replaces triphylite, and heterosite replaces ferrisicklerite following a chemical process of Li leaching and progressive oxidation of transition cations with almost constant Fe/(Fe + Mn) values (Quensel 1937, Mason 1941, Fransolet *et al.* 1985, Fransolet 2007). The origin of kryzhanovskite is unclear; in fact, textural characteristics relate this mineral to ferrisicklerite even if the Fe/(Fe + Mn) value of 0.77 is lower than that of ferrisicklerite. Similar considerations are suitable even for staněkite, which appears to replace ferrisicklerite mainly along fractures and to be replaced by heterosite; its Fe/(Fe + Mn) value of 0.69 is consistent with that of graftonite. The sequence of crystallization of association I is outlined in Figure 6A.

In all samples found at Brissago, association I is completely or almost completely overrun by association II. Only small relics of the magmatic association are still preserved in the core of the phosphate masses. Polycrystalline texture of association II indicates a pervasive process of recrystallization, which involved association I after its complete crystallization. Generally, these dramatic changes in texture of phosphates are attributed to metasomatic processes, which are accompanied by strong changes of mineral associations and chemical composition (Moore 1973, Fransolet *et al.* 1986, and references therein). At Brissago, no significant changes in mineralogical composition and chemical features of the assemblage of primary phosphates were detected between association I and association II, except for a

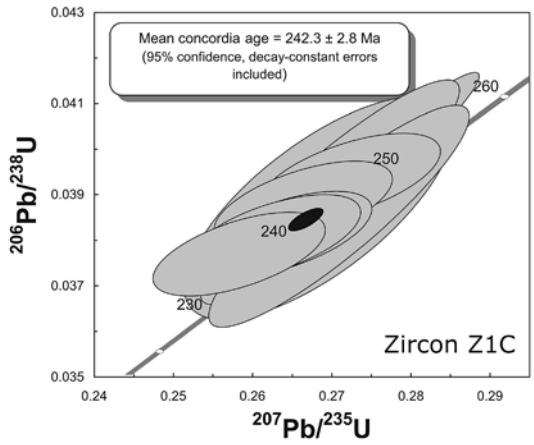

FIG. 5. A $^{207}Pb/^{235}U - ^{206}Pb/^{235}U$ concordia diagram with the mean concordia age from zircon crystals taken from the Brissago phosphate-bearing pegmatite of the ZPU boulder (data-point error ellipses are 2σ).

negligible amount of maghagendorfite in polycrystalline masses. For these reasons, we infer that association II formed through an autometamorphic textural rearrangement of association I under isochemical conditions. This hypothesis is confirmed by the geochronological data of zircon. The postmagmatic resetting of the U–Pb system at 219.5 ± 9.9 and 229 ± 10 Ma (2σ) point to reheating episodes involving the pegmatite. The reheating led the metamorphic rearrangement of the phosphate minerals association. We believe that the association jahnsite–mitridatite locally replaced graftonite during late metamorphic processes as a result of Ca diffusion from the nearby apatite at the rim of polycrystalline phosphate masses. Processes of hydrothermal alteration are limited and occurred mainly as progressive hydroxylation and Li-leaching in non-oxidizing conditions, with the replacement of ludlamite at the expense of triphylite and with the crystallization of vivianite. The sequence of crystallization of association II is outlined in Figure 6B.

The origin of the pegmatite-forming melt

The U/Pb age of 242 ± 2.8 Ma obtained from the two crystals of zircon extracted from the ZPU boulder, allow us to associate the emplacement of phosphate-bearing pegmatites to the onset of the Mid-Triassic tectonomagmatic cycle (top of Anisian – base of Ladinian; Brack *et al*. 2005), well represented in the whole Southern Alps. In contrast, the common dioritic and granitic dikes, cropping out in the higher part of Valle di Ponte, are related to the Early Permian magmatic cycle, as established by Mulch *et al*. (2002). No data exist about the age of emplacement of the phosphate-free granitic pegmatites, and field evidence does not allow us to link them to any magmatic cycle. Therefore, a parent

TABLE 6. ISOTOPIC RATIOS AND APPARENT AGES OF ZIRCON SAMPLES Z1C2 AND Z1C3

Sample	Isotope ratios						Apparent ages					
	$^{207}Pb/^{206}Pb$	1σ	$^{206}Pb/^{238}U$	1σ	$^{207}Pb/^{235}U$	1σ	concordia age	2σ	$^{206}Pb/^{238}U$	1σ	$^{207}Pb/^{235}U$	1σ
Z1C3-1	0.05012	0.001	0.0394	0.0004	0.2722	0.005	248.6	4.9	249.0	2.5	244.4	4.2
Z1C3-2	0.05003	0.001	0.0380	0.0004	0.2625	0.005	240.4	4.8	240.7	2.5	236.7	4.1
Z1C3-3	0.04959	0.001	0.0399	0.0004	0.2729	0.005	---	---	252.2	2.5	245.0	4.2
Z1C3-4	0.05019	0.001	0.0381	0.0004	0.2638	0.005	240.9	4.8	241.1	2.5	237.7	4.1
Z1C3-5	0.04969	0.001	0.0377	0.0004	0.2581	0.004	238.0	4.7	238.4	2.4	233.2	4.0
Z1C3-6	0.04979	0.001	0.0388	0.0004	0.2663	0.005	244.8	4.8	245.3	2.5	239.7	4.1
Z1C2-1	0.05034	0.001	0.0408	0.0011	0.2814	0.007	---	---	257.5	6.7	251.8	6.3
Z1C2-2	0.05067	0.001	0.0387	0.0010	0.2682	0.007	242.0	11.0	244.7	6.4	241.2	6.3
Z1C2-3	0.05126	0.001	0.0385	0.0010	0.2708	0.007	243.0	11.0	243.6	6.3	243.3	6.1
Z1C2-4	0.05029	0.001	0.0349	0.0009	0.2402	0.006	219.5	9.9	220.8	5.8	218.6	5.9
Z1C2-5	0.04992	0.001	0.0398	0.0010	0.2722	0.007	---	---	251.4	6.5	244.5	6.0
Z1C2-6	0.05038	0.001	0.0394	0.0010	0.2722	0.007	---	---	249.3	6.5	244.5	6.1
Z1C2-7	0.05038	0.001	0.0390	0.0010	0.2697	0.007	241.0	11.0	246.9	6.4	242.4	6.0
Z1C2-8	0.05033	0.001	0.0367	0.0010	0.2520	0.006	229.0	10.0	232.5	6.1	228.2	5.9
Z1C2-9	0.04694	0.001	0.0357	0.0009	0.2308	0.006	---	---	226.2	6.0	210.9	5.3
Z1C2-10	0.05051	0.001	0.0392	0.0010	0.2721	0.007	240.0	9.8	247.8	6.5	244.4	6.0

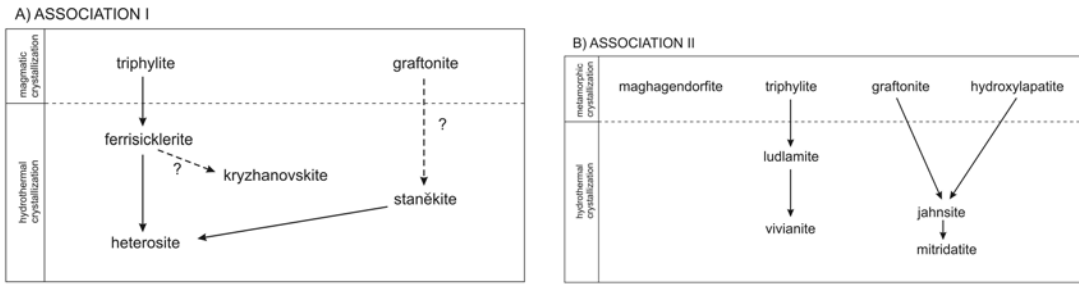

FIG. 6. Alteration sequence of phosphate minerals: A) association I; B) association II.

granite for the phosphate-bearing pegmatites is missing in the Brissago – Valle di Ponte area. As discussed above, the Brissago phosphate-bearing pegmatites are poorly fractionated and geochemically primitive. Large amounts of plagioclase (mainly albite with minor oligoclase near the contact with the host rock) and muscovite indicate a peraluminous character of the pegmatite-forming melt, whereas the abundance of schorl suggests an appreciable content of boron. These geochemical characteristics indicate that the pegmatite-forming melt originated in a primitive geological environment, as proposed for the Conifer Road pegmatite, in northwestern Ontario, by Černý *et al.* (1998). We contend that the phosphate-bearing pegmatites at Brissago crystallized from a poorly evolved melt probably produced by local partial melting of kinzigites during the high-temperature metamorphic process and hydration induced by the hydrothermal plume rising from the subducting plate. In this environment the peraluminous character of the melt could be inherited from kinzigites, that can also be considered the source for B, Li and P (Martin & De Vito 2005).

Acknowledgements

We acknowledge E. Garzanti, F. Pezzotta, G. Vezzoli and S. Andò for helpful suggestions. The authors are particularly grateful to R.F. Martin, M.-L. Sirbescu, E. Roda and an anonymous reviewer for their constructive comments and detailed review of the submitted manuscript. This work was financially supported by the "Museo Cantonale di Storia Naturale" (Lugano, Switzerland) and by the Istituto per la dinamica dei processi ambientali (IDPA) of the Italian National Research Council (CNR) (Research Project P1–01: "Geodynamics and evolution of continental lithosphere"). We also thank the CNR – Istituto per la dinamica dei processi ambientali for providing facilities for chemical analysis.

References

Bertotti, G., Seward, D., Wijbrans, J., ter Voorde, M. & Hurford, A.J. (1999): Crustal thermal regime prior to, during, and after rifting: a geochronological and modelling study of the Mesozoic South Alpine rifted margin. *Tectonics* **18**(2), 185-200.

Boriani, A., Burlini, L. & Sacchi, R. (1990): The Cossato-Mergozzo-Brissago Line and the Pogallo Line (Southern Alps, northern Italy) and their relationships with the late-Hercynian magmatic and metamorphic events. *Tectonophysics* **182**, 91-102.

Boriani, A., Caironi, V., Giobbi Origoni, E. & Vannucci R. (1992): The Permian intrusive rocks of Serie dei Laghi (Western Southern Alps). *Acta Vulcanologica* **2**, 73-86.

Boriani, A. & Sacchi, R. (1973): Geology of the junction between the Ivrea–Verbano and Strona–Ceneri zones (Southern Alps). *Mem. Istituto Geol. Mineral. Padova* **28**, 1-35.

Brack, P., Rieber, H., Nicora, A. & Mundil, R. (2005): The global boundary stratotype section and point (GSSP) of the Ladinian stage (Middle Triassic) at Bagolino (Southern Alps, northern Italy) and its implications for the Triassic time scale. *Episodes* **28**, 233-244.

Cavalli, I. (1984): *Mineralogische Untersuchungen an Graftoniten aus Sudalpinen Pegmatiten (Olgiasca, Italien und Brissago, TI).* Doctoral Thesis, University of Basel, Basel, Switzerland.

Černý, P. & Ercit, T.S. (2005): The classification of granitic pegmatites revisited. *Can. Mineral.* **43**, 2005-2026.

Černý, P., Selway, L.B., Ercit, T.S., Breaks, F.W., Anderson, A.J. & Anderson, S.D. (1998): Graftonite–beusite in granitic pegmatites of the Superior Province: a study in contrasts. *Can. Mineral.* **36**, 367-376.

De Quervain, F. (1932): Pegmatitbildungen von Valle della Madonna bei Brissago. *Mitt. nat. Ges.* **3**, 10-24.

Fleischer, M., Cabri, L.J., Chao, G.Y. & Pabst, A. (1980): New mineral names. *Am. Mineral.* **65**, 808-814.

Fountain, M.D. (1976): The Ivrea–Verbano and Strona–Ceneri Zones, northern Italy: a cross-section of the continental crust – new evidence from seismic velocities of rock samples. *Tectonophysics* **33**, 145-165.

Fransolet, A.M. (2007): Phosphate associations in the granitic pegmatites: the relevant significance of these accessory minerals. *In* Granitic Pegmatites: the State of the Art, an International Symposium (T. Martins & R. Vieira, eds.). *Universidade do Porto, Departemento de Geologia, Memorias* **8**, 102-103.

Fransolet, A.-M., Abraham, K. & Speetjens, J.M. (1985): Evolution génétique et signification des associations de phosphates de la pegmatite d'Angarf-Sud, plaine de Tazenakht, Anti-Atlas, Maroc. *Bull. Minéral.* **108**, 551-574.

Fransolet, A.-M., Hatert, F. & Fontan, F. (2004): Petrographic evidence for primary hagendorfite in an unusual assemblage of phosphate minerals, Kibingo granitic pegmatite, Rwanda. *Can. Mineral.* **42**, 697-704.

Fransolet, A.-M., Keller, P. & Fontan, F. (1986): The phosphate mineral associations of the Tsaobismund pegmatite, Namibia. *Contrib. Mineral. Petrol.* **92**, 502-517.

Furin, S., Preto, N., Rigo, M., Roghi, G., Gianolla, P., Crowley, J.L. & Bowring, S.A. (2006): High precision U–Pb zircon age from the Triassic of Italy: implications for the Triassic time scale and the Carnian origin of calcareous nanoplankton and dinosaurs. *Geology* **34**, 1009-1012.

GAETANI, M., GNACCOLINI, M., JADOUL, F. & GARZANTI, E. (1998): Multiorder sequence stratigraphy in the Triassic system of the western Southern Alps. *In* Mesozoic and Cenozoic Sequence Stratigraphy of European Basins (P.C. de Graciansky, J. Hardenbol, T. Jacquin & P.R. Vail, eds.). *SEPM, Spec. Publ.* **60**, 701-717.

GARZANTI, E. (1985): The sandstone memory of the evolution of a Triassic volcanic arc in the Southern Alps, Italy. *Sedimentology* **32**, 423-433.

GARZANTI, E., ANDÒ, S. & VEZZOLI, G., (2006): The continental crust as a source of sand (Southern Alps cross-section, northern Italy). *J. Geol.* **114**, 533-554.

GARZANTI, E., GNACCOLINI, M. & JADOUL, F. (1995): Anatomy of a semiarid coastal system: the Upper Carnian of Lombardy. *Riv. Ital. Paleontol. Stratigr.* **101**, 17-36.

GARZANTI, E., SCIUNNACH, D. & CONFALONIERI, M. (2003): Discriminating source rock and environmental control from detrital models of Permo-Triassic fluvio-deltaic sandstones. I. Southern Alps (Lombardy, Italy). *In* Quantitative Provenance Studies in Italy (R.Valloni & A. Basu, eds.). *Memorie descrittive della Carta Geologica d'Italia* **61**, 63-82.

GIESE, P. (1968): Die Struktur der Erdkruste im Bereich der Ivrea-Zone. Ein Vergleich verschiedener, seismischer Interpretationen und der Versuch einer petrographisch-geologischen Deutung. *Schweiz. Mineral. Petrogr. Mitt.* **48**, 261-284.

GRIECO, G., FERRARIO, A., VON QUADT, A., KOPPEL, V. & MATHEZ, E.A. (2001): The zircon-bearing chromitites of the phlogopite peridotite of Finero (Ivrea Zone, Southern Alps): evidence and geochronology of a metasomatized mantle slab. *J. Petrol.* **42**, 89-101.

GUASTONI, A., NESTOLA, F., MAZZOLENI, G. & VIGNOLA, P. (2007): Mn-rich graftonite, ferrisicklerite, stanĕkite and Mn-rich vivianite in a granitic pegmatite at Soè Valley, central Alps, Italy. *Mineral. Mag.* **71**, 579-585.

HANDY, M.R. (1986): *The Structure and Rheological Evolution of the Pogallo Fault Zone, a Deep Crustal Dislocation in the Southern Alps of Northwestern Italy (Prov. Novara).* Doctoral Thesis, University of Basel, Basel, Switzerland.

HANDY, M.R. (1987): The structure, age and kinematics of the Pogallo Fault Zone, Southern Alps, northwestern Italy. *Eclogae Geol. Helv.* **80**, 593-632.

HATERT, F., KELLER, P., LISSNER, F., ANTENUCCI, D. & FRANSOLET, A.-M. (2000): First experimental evidence of alluaudite-like phosphates with high Li-content: the $(Na_{1-x}Li_x)MnFe_2(PO_4)_3$ series (x = 0 to 1). *Eur. J. Mineral.* **12**, 847-857.

HEITZMANN, P. (1987): Relationships between the Alpine suture and the Insubric line in the Central Alps: structural, geochronological and geophysical evidences. *Int. Conf. Deformation & Plate Tectonics* (*Gijon – Oviedo*), *Abstr.*

HORSTWOOD, M.S.A., FOSTER, G.L., PARRISH, R.R., NOBLE, S.R. & NOWELL, G.M. (2003). Common-Pb corrected in situ U–Pb accessory mineral geochronology by LA–MC–ICP–MS. *J. Anal. At. Spectr.* **18**, 837-846.

HURLBUT, C.S., JR. (1965): Detailed description of sarcopside from East Alstead, New Hampshire. *Am. Mineral.* **50**, 1698-1707.

JADOUL, F., BERRA, F. & FRISIA, S. (1992): Stratigraphic and paleogeographic evolution of a carbonate platform in an extensional tectonic regime: the example of the Dolomia Principale in Lombardy (Italy). *Riv. Ital. Paleontol. Stratigr.* **98**, 29-44.

KELLER, P. & VON KNORRING, O. (1989): Pegmatites at the Okatjimukuju farm, Karibib, Namibia. I. Phosphate mineral associations of the Clementine II pegmatite. *Eur. J. Mineral.* **1**, 567-593.

LONDON, D., WOLF, M.B., MORGAN, G.B., VI & GALLEGO GARRIDO, M. (1999): Experimental silicate–phosphate equilibria in peraluminous granitic magmas, with a case study of the Albuquerque batholith at Tres Arroyos, Badajoz, Spain. *J. Petrol.* **40**, 215-240.

LU, MEIHUA, ALBRECHT, H.W., MAZZUCCHELLI, M. & RIVALENTI, G. (1997): The mafic-ultramafic complex near Finero (Ivrea–Verbano Zone). II. Geochronology and isotope geochemistry. *Chem. Geol.* **140**, 223-235.

LUDWIG, K.R. (2000): Users Manual for Isoplot/Ex: A Geochronological Toolkit for Microsoft Excel. *Berkeley Geochronology Center, Spec. Publ.*

MARINELLI, M., VIEL, G. & FARABEGOLI, E. (1980): Il Permo-Trias delle Alpi Meridionali: evoluzione tardo-ercinica di un bacino marginale di retroarco ensialico. *Ind. Mineraria* **6**, 1-14.

MARTIN, R.F. & DE VITO, C. (2005): The patterns of enrichment in felsic pegmatites ultimately depend on tectonic setting. *Can. Mineral.* **43**, 2027-2048.

MASON, B. (1941): Minerals of the Varuträsk pegmatite. XXIII. Some iron–manganese phosphate minerals and their alteration products, with special reference to material from Varuträsk. *Geol. Fören. Stockholm Förh.* **63**, 117-175.

MEISSER, N. & VANINI, F. (1997): Neues zur Mineralogie der Pegmatite des Valle di Ponte, Brissago (TI). *Schweizer Strahler* **11**(1), 42-44.

MOORE, P.B. (1971): Crystal chemistry of the alluaudite structure type: contribution to the paragenesis of pegmatite phosphate giant crystals. *Am. Mineral.* **56**, 1955-1975.

MOORE, P.B. (1973): Pegmatite phosphates: descriptive mineralogy and crystal chemistry. *Mineral. Rec.* **4**, 103-130.

MOORE, P.B. & ITO, J. (1979): Alluaudites, wyllieites, arrojadites: crystal chemistry and nomenclature. *Mineral. Mag.* **43**, 227-235.

MULCH, A., ROSENAU, M., DÖRR, W. & HANDY, M.R. (2002): The age and structure of the dikes along the tectonic contact of the Ivrea–Verbano and Strona–Ceneri zones (Southern Alps, northern Italy, Switzerland). *Schweiz. Mineral. Petrogr. Mitt.* **82**, 55-76.

MUNDIL, R., BRACK, P., MEIER, M., RIEBER, H. & OBERLI, F. (1996): High resolution U/Pb dating of the Middle Triassic volcaniclastics: time-scale calibration and verification of tuning parameters for carbonate sedimentation. *Earth Planet. Sci. Lett.* **141**, 137-151.

NYFFELER, M. (1972): Die Pegmatite der Region Brissago. *Schweizer Strahler* **2**(9), 312-313.

OPPIZZI, P. & SCHALTEGGER, U. (1999): Zircon bearing plagioclasites from the Finero complex (Ivrea Zone): dating a Late Triassic mantle. *Schweiz. Mineral. Petrogr. Mitt.* **79**, 330-331.

PEZZOTTA, F., DIELLA, V. & GUASTONI, A. (2005): Scandium silicates from the Baveno and Cuasso al Monte NYF-granites, Southern Alps (Italy): mineralogy and genetic inferences. *Am. Mineral.* **90**, 1442-1452.

QUENSEL, P. (1937): Minerals of the Varuträsk pegmatite. I. The lithium–manganese phosphates. *Geol. Fören. Stockholm Förh.* **59**, 77-96.

RODA, E., PESQUERA, A., FONTAN, F. & KELLER, P. (2004): Phosphate mineral associations in the Cañada pegmatite (Salamanca, Spain): paragenetic relationships, chemical compositions, and implications for pegmatite evolution. *Am. Mineral.* **89**, 110-125.

SANDERS, C.A.E., BERTOTTI, G., TOMMASINI, S., DAVIES, G.R. & WIJBRANS, J.R. (1996): Triassic pegmatites in the Mesozoic middle crust of the Southern Alps (Italy): fluid inclusions, radiometric dating and tectonic implications. *Eclogae Geol. Helv.* **89**, 505-525.

SCHMID, S.M., ZINGG, A. & HANDY, M. (1987): The kinematics of movements along the Insubric Line and the emplacement of the Ivrea Zone. *Tectonophysics* **135**, 47-66.

SILETTO, G.B., SPALLA, M.I., TUNESI, A., LARDEAUX, J.M. & COLOMBO, A. (1993): Pre-alpine structural and metamorphic histories in the Orobic Southern Alps, Italy. *In* Pre-Mesozoic Geology in the Alps (J.F. Von Raumer & F. Nebauer, eds.). Springer-Verlag, Berlin, Germany (585-598).

SIMMONS, W.B., WEBBER, K.L., FALSTER, A.U. & NIZAMOFF, J.W. (2003): *Pegmatology: Pegmatite Mineralogy, Petrology & Petrogenesis*. Rubellite Press, New Orleans, Louisiana.

SMEDS, S.A., HUER, P., Černý, P., WISE, M.A., GUSTAFSSON, L. & PENNER, P. (1998): Graftonite–beusite in Sweden: primary phases, products of exsolution, and distribution in zoned populations of granitic pegmatites. *Can. Mineral.* **36**, 377-394

STAMPFLI, G., MARCOUX, J. & BAUD A. (1991): Tethyan margins in space and time. *In* Paleogeography and Paleoceanography of Tethys (W. Cavazza *et al.*, eds.). *Palaeogeography, Palaeoclimatology, Palaeoecology* **87**, 373-409.

TIEPOLO, M. (2003). In situ Pb geochronology of zircon with laser ablation – inductively coupled plasma – sector field mass spectrometry. *Chem. Geol.* **199**, 159-177.

VAN ACHTERBERGH, E., RYAN, C.G., JACKSON, S.E. & GRIFFIN, W. (2001): Data reduction software for LA–ICP–MS. *In* Laser Ablation – ICPMS in the Earth Sciences (P. Sylvester, ed.). *Mineral. Assoc. Can., Short Course Vol.* **29**, 239-243.

WALTER, P. (1950): *Das Ostende der Ivrea–Verbano und Tessiner Wurzelzone*. Doctoral Thesis, ETH, Zürich, Switzerland.

WEISS, S. (1982): Pegmatitmineralien von Brissago (TI). *Lapis* **7**(7-8), 48-55.

WEISS, S. (1985): Neufunde und Neubestimmungen von Brissago/Tessin. *Lapis* **9**(4), 23-24.

WEISS, S. (1989): Columbit und Jahnsit aus Brissago (TI). *Lapis* **14**(6), 33-37.

WEISS, S., VIGNOLA, P., DIELLA, V., MEISSER, N., OPPIZZI, P. & GRUNDMANN, G. (2004): Die Mineralien der Pegmatite von Brissago, Tessin, Schweiz: außergewöhnliche Neufunde 1999–2001. *Lapis* **29**, 24-38.

WIDENBECK, M., ALLÉ, P., CORFU, F., GRIFFIN, W.L., MEIER, M., OBERLI, F., VON QUADT, A., RODDICK, J.C. & SPIEGEL, W. (1995): Three natural zircon standards for U–Th–Pb, Lu–Hf, trace element and REE analysis. *Geost. Newslett.* **19**(1), 1-23.

WISE, M.A. & Černý, P. (1990): Beusite–triphylite intergrowths from the Yellowknife pegmatite field, Northwest Territories. *Can. Mineral.* **28**, 133-139.

ZINGG, A. & HUNZIKER, J.C. (1990): The age of movements along the Insubric Line West of Locarno (northern Italy and southern Switzerland). *Eclogae geol. Helv.* **83**, 629-644.

Received July 18, 2007, revised manuscript accepted May 20, 2008.